

## Classification of Different Type of Propeller Ventilation and Ventilation Inception Mechanism

Anna M. Kozłowska<sup>1,3</sup>, Sverre Steen<sup>1,3</sup> and Kourosh Koushan<sup>2</sup>

<sup>1</sup>Department of Marine Technology, Norwegian University of Science and Technology (NTNU), Trondheim, Norway

<sup>2</sup>Norwegian Marine Technology Research Institute (MARINTEK), Trondheim, Norway

<sup>3</sup>Rolls-Royce University Technology Centre "Performance in a Seaway" Trondheim, Norway

### ABSTRACT

The paper is largely based on analysis of a series of experiments by Koushan (2006 I and II), where an azimuth thruster with open propeller is tested in conditions with intermittent ventilation. The use of a 6-component blade dynamometer on one of the four propeller blades gives detailed insight into the forces on the propeller, while the use of high-speed underwater video gives a visual understanding of the ventilation phenomena. Analysis of the propeller ventilation can be divided in two parts: aiming at classification of different types of propeller ventilation and typical thrust loss related to each of them, and the discussion of the ventilation inception mechanism based on the requirements for propeller to ventilate: i.e. propeller loading, forward speed and submergence.

### Keywords

Intermittent ventilation, thrust losses, torque variations, thrusters.

### 1 INTRODUCTION

Thruster propellers are used as maneuvering, dynamic positioning and main propulsion units and very often works in heavy sea conditions. In that case, thrusters subject to propeller ventilation (when air is drawn into the propeller flow) may experience large loss of propeller thrust and possibly damaging dynamic loads as well as noise and vibration. It seems that more knowledge is needed to understand the typical magnitude of thrust loss and dynamic forces related to the different types of ventilation. The overall goal of this work is to get a firm understanding of the fluid load mechanisms resulting in large and rapid changes in the propeller loading and also showing how to avoid the more harmful types of propeller ventilation, either by design requirements or by operational guidance for ships when operating in off design conditions.

Propulsion dynamics due to inflow angle onto the propeller, speed of the flow, propeller emergence and ventilation have been studied experimentally as well as theoretically by several researchers since 1933 see e.g.

Kempf (1933), Shiba (1953), Fleischer (1973), Faltinsen (1981, 1983), Minsaas (1975, 1981, 1983), Olofsson (1996) and Koushan (2006). Kempf (1933) was one of the first researchers who studied the ventilation effect on propellers. He studied the torque and thrust loss due to ventilation using three similar propellers of different diameters as well as different immersion ratios and propeller rate of revolutions. Ventilation effect on thrust and torque was also study by Shiba (1953), who discussed the influence of different propeller design parameters e.g. expanded area ratio, contour of blade, radial variation of pitch, skewback, effect of rudder, turbulence of original flow as well as scale effects on ventilation. Ventilation effects with respect to vessel operation in addition to added resistance in waves and reduction of propulsive efficiency can be found in Faltinsen (1981, 1983) and Minsaas (1975, 1981, and 1983). Olofsson (1996) studied the force and flow characteristics of surface piercing propellers. Koushan (2006) has performed extensive model tests on an azimuth thruster with 6 DoF measurements of forces on one of the four blades reported in three papers (Koushan 2006 I, II and III). In model experiments different conditions were tested. Propeller immersion ratio, carriage speed, propeller rate of revolution, azimuth angle, period of heave oscillations, oscillations amplitude, type of propeller (open and ducted) and propulsion (pulling and pushing) were varied during the experiments. It is anticipated that these experiments contain a lot of information which have not been utilised yet and new analysis should be performed in order to get understanding of the physics of the fluid load mechanism causing thrust losses and torque variations.

Koushan (2006 I) described the dynamics of ventilated propeller blade axial force on pulling thruster at bollard condition running at several constant immersion ratios and constant propeller rate of revolution.

Koushan (2006 II) presented the dynamics of ventilated propeller blade axial force on pulling thruster at bollard condition and constant propeller rate of revolution moving with forced sinusoidal heave motion.

Koushan (2006 III) presented the dynamics of ventilated propeller blade and duct loadings at bollard condition and constant propeller rate of revolution.

The aim of this paper is to systematise the different types of ventilation appearing on propellers at low advance ratios, and to discuss the thrust loss related to each of them. We have also studied how well the thrust loss is predicted by existing formulas. This paper is based on systematic model tests performed by Koushan (2006 I and II) of an open propeller subject to intermittent ventilation. Shaft speed, submergence ratio and advance speed were varied during these experiments.

Scaling laws for ventilating propellers are presented in section 3. In sections 4 & 5 the paper focuses on classification of different kind of ventilation inception mechanisms and also separates ventilation phenomena in three different regimes. In sections 6 & 7 the authors concentrate on the average thrust and torque loss due to ventilation and out of water effects. The relation between the thrust and torque loss factors are presented and compared with empirical formulas. In the last section the paper focuses of thrust loss due to blade position with the help of visual observations based on photographs taken by an underwater high speed camera. All photographs, which are presented in this paper, show the suction side of the propeller.

## SYMBOLS INDEX

$A_0$	$[m^2]$	propeller disc area
$A_{wet}$	$[m^2]$	wetted propeller disc area
$c$	$[m]$	chord length
$c_L$	$[-]$	lift coefficient
$D, R$	$[m]$	propeller diameter/radius
$EAR$	$[-]$	blade area ratio
$F_{nh}$	$[-]$	depth Froude's number
$h$	$[m]$	submergence of propeller shaft
$J_M, J_F$	$[-]$	advance ratio in model and full scale
$J$	$[-]$	advance ratio
$K_{Q_n}$	$[-]$	nominal torque coefficient
$K_{Q_t}$	$[-]$	total torque coefficient
$K_{T_n}$	$[-]$	nominal thrust coefficient
$K_{T_t}$	$[-]$	total thrust coefficient
$L_M, L_F$	$[m]$	characteristic length in model/full scale
$n$	$[Hz]$	shaft speed per second
$p_{at}$	$[Pa]$	atmospheric pressure
$p_{cav}$	$[Pa]$	pressure in cavity
$Q_n$	$[Nm]$	nominal torque (no ventilation)
$Q_t$	$[Nm]$	total torque
$R_e$	$[-]$	Reynold's number

$S$	$[N/m]$	surface tension of the water
$T_n$	$[N]$	nominal thrust (no ventilation)
$T_t$	$[N]$	total thrust
$V$	$[m/s]$	advance speed
$V_\infty$	$[m/s]$	velocity seen by propeller blade at 0.7 R
$We$	$[-]$	Weber's number
$z$	$[-]$	number of blades
$\alpha$	$[deg]$	angle of attack
$\beta$	$[-]$	thrust loss without the effect of ventilation
$\beta_0$	$[-]$	thrust loss due to loss of propeller disc area
$\beta_T, \beta_Q$	$[-]$	total thrust/torque loss factors
$\beta_V$	$[-]$	thrust loss for fully ventilated propeller due to ventilation
$\beta_W$	$[-]$	thrust loss due to Wagner effect
$\beta_{WAVE}$	$[-]$	thrust loss due to wave making by propeller
$\lambda$	$[-]$	scale
$\nu$	$[m^2/s]$	kinematic viscosity of the water
$\rho$	$[kg/m^3]$	density of water
$\sigma$	$[-]$	cavitation or ventilation number
$\sigma_V$	$[-]$	ventilation number
FS		Free surface

## 2 TEST SET UP AND INSTRUMENTATION

The experiments were conducted in Marine Cybernetics Laboratories at the Norwegian University of Science and Technology. This tank is 40 m long, 6.45 m wide and 1.5 m deep. The four bladed, right handed open propeller was mounted on a pulling thruster. In order to capture the dynamics a high sampling frequency of 2400Hz was used during experiments. The propeller has a diameter of 250 mm, design pitch ratio of 1.1 and expanded area ratio of 0.595. For more detailed description see (Koushan 2006 I). Blade axial, radial, tangential forces and moments about all three axes were measured during the experiments. A pulse meter provided propeller rate of revolutions as well as indicating the angular position of the reference blade.

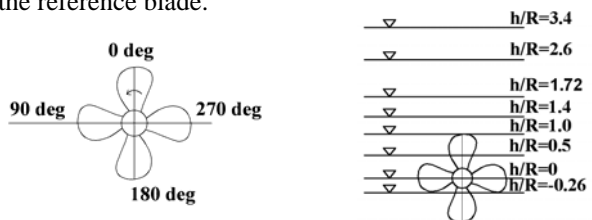


Figure 1 Blade position

Figure 2 Submergence ratios

For partially submerged propellers we can divide one blade cycle (from 0 to 360 deg) in four phases: 1<sup>st</sup> the blade entry phase, 2<sup>nd</sup> the in - water phase, 3<sup>rd</sup> the blade

exit phase and 4<sup>th</sup> the in - air phase. The blade entry phase starts when the blade touches the free surface and finishes when the whole blade is submerged. The continuation of the blade entry phase is the in - water phase. The blade water phase is followed by blade exit phase, which starts when the leading edge of the blade touches the free surface and terminates when the whole blade is in the in - air phase.

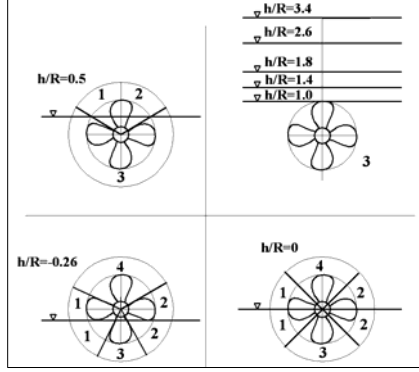


Figure 3 Blade cycle phase, 1- the blade entry phase, 2- the blade exit phase, 3- the in water phase, and 4 - the in air phase

### 3 SCALE EFFECTS ON VENTILATION

In order to scale the propeller performance from model tests to full scale the following conditions have to be fulfilled:

#### 3.1 Geometrical similarity

$$\lambda = \frac{L_F}{L_M} \quad (1)$$

Where index  $M$  means model scale and index  $F$  means full scale,  $L_M$  and  $L_F$  are respectively any dimension in model and full scale.

#### 3.2 Kinematic similarity

$$J_F = \frac{V_F}{n_F D_F} = \frac{V_M}{n_M D_M} = J_M \quad (2)$$

#### 3.3 Dynamic similarity

To fulfill dynamic similarity the ratios between forces in model scale have to be equal to corresponding ratios in full scale. The forces of importance are inertia and gravitational forces (Froude's number), viscous forces (Reynold's number), inertia and surface tension forces (Weber's number) as well as cavitation and ventilation number.

Reynold's number:

$$R_{n,0.7} = \frac{V_\infty c(0.7)}{v} \quad (3)$$

$$V_\infty = \sqrt{V^2 + (0.7\pi nD)^2} \quad (4)$$

depth Froude's number:

$$F_{nh} = \frac{\pi nD}{\sqrt{gh}} \quad (5)$$

Weber's number: 
$$We = nD \sqrt{\frac{\rho D}{S}} \quad (6)$$

Cavitation and ventilation number:

$$\sigma = \frac{p_{at} + \rho gh - p}{\frac{1}{2} \rho V_\infty^2} \quad (7)$$

Where:  $p = p_{at}$  for ventilation,  $p = p_{cav}$  for cavitation.

Reynold's number dependence for deeply submerged propeller as well as when propellers working near the free surface can be neglected at Reynold's numbers above the so-called minimum Reynold's number, which is  $3 \cdot 10^5$  acc. to Minsaas (1975). For Koushan model tests only for the lowest propeller speed the influence of Reynolds scale effect is likely to be of importance. For propeller revolution over  $n=6\text{Hz}$ , Reynolds number dependence can be neglected.

The influence of wave making by the propeller becomes of importance (Froude's number) when a propeller is close to the free surface or coming out of the water. In order to model of the wave making correctly depth Froude's number must be identical for model and full scale, and this requirement is actually fulfilled through kinematic similarity and submergence ratio similarity.

According to Shiba (1953) the influence of Weber's number disappears above the so-called minimum Weber's number, which is about 180. Full scale propellers usually operate above Weber's number 180 but for model scale tests Weber's number could be lower than minimum values. In our case only for propeller revolution over  $n=13\text{Hz}$ , the influence of Weber's number can be neglected.

When the propeller is fully ventilated the pressure on the suction side of the propeller blade is atmospheric. Ventilation number is defined as follows:

$$\sigma_V = \frac{p_{at} + \rho gh - p_{at}}{\frac{1}{2} \rho V_\infty^2} = \frac{2gh}{V_\infty^2} \quad (8)$$

For given advance ratio ventilation number similarity is satisfied if depth Froude's number similarity is fulfilled which means that ventilation number similarity is satisfied when submergence ratio and kinematic similarity is fulfilled.

For the non ventilated regime, the extent of cavitation in full scale should not be sufficient to significantly influence the thrust and torque, so for our study of ventilation and thrust loss, not satisfying the cavitation number similarity for non-ventilating conditions is not considered a problem. When the propeller operates in fully ventilated regime, all low pressure areas can be expected to be ventilated before they cavitate, so cavitation number similarity is not required. For partially ventilated condition, there might be a link between cavitation and ventilation inception, so for this condition, not satisfying cavitation number similarity is questionable. Based on the discussion above the conclusion is that for non ventilated and fully ventilated regime the results from model tests performed by Koushan are scalable from model to full scale, while in

partially ventilated regime the results are not necessarily scalable due to the possible influence of cavitation in full scale.

#### 4 VENTILATION INCEPTION MECHANISM

Ventilation inception depends on different parameters i.e. propeller loading, forward speed, propeller submergence and time. Based on these requirements for the propeller to ventilate, ventilation inception mechanism can be divided in three conditions.

For condition I ventilation always starts by forming an air filled vortex from the free surface as illustrated in Figure 4. The vortex acts on the suction side on the propeller, the pressure side is probably free of ventilation. The vortex funnel can appear on the surface quite far from the propeller disc, especially for large submergence ratios. The appearance of a vortex funnel is a time dependent phenomena. It also depends on the forward speed of the propeller. For high advance ratios the vortex can be suppressed by the flow around the propeller.

Condition I corresponds to  $1.4 \leq h/R \leq 3.4$ , low positive and negative forward speeds as well as bollard condition, propeller revolutions:  $n < 9\text{Hz}$  for propeller submergence  $h/R=1.4$  and propeller revolutions:  $n \geq 5\text{Hz}$  for propeller submergence  $1.4 < h/R < 3.4$ . For propeller revolutions less than 9Hz and propeller submergence equal to 3.4 ventilation phenomena do not occur during the model test.

Condition III is observed for less submergence than  $0.4R$  from tip to free surface, which correspond to  $h/R < 1.4$ . Ventilation starts when the propeller starts rotating; the free surface is sucked down to the propeller.

Condition II lay between condition I & III. Ventilation in this case starts probably by forming the air filled vortex from the free surface but it is hard to observe, due to the blade, which crosses the vortex and partially destroys it, producing a lot of air bubbles, which makes observations more difficult. Conditions II and III are illustrated in Figure 5.

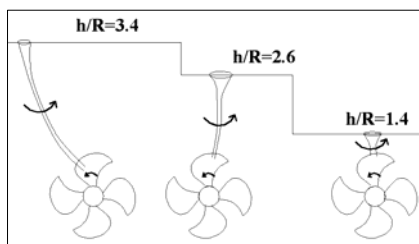


Figure 4 Condition I

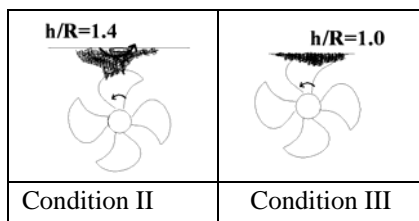


Figure 5 Conditions II & III

For propeller submergence not less than 1.4, which corresponds with condition I & II the propeller operates

in partially and fully ventilated regimes. As a result the thrust loss is much lower if we compare with condition III, which correspond to fully ventilated regime.

#### 5 DIFFERENT VENTILATION REGIMES

Ventilation phenomena can be separated in three different time dependent regimes: ventilation inception, partial ventilation and full ventilation.

For condition I i.e. deeply submerged propellers and low or zero advance ratios, ventilation starts by forming the air filled vortex from the free surface. Between fully ventilated regime and partially ventilated regime the propeller reaches the transition region, when the ventilation changes from partial to full ventilation - see Figure 6.

For condition II the ventilation inception regime takes less time compared to condition I, and changes rapidly first to partially ventilated regime and second to fully ventilated case.

For condition III only fully ventilated regime was detected. Ventilation starts when the propeller starts rotating and we observe larger drop in thrust compared with condition I and II.

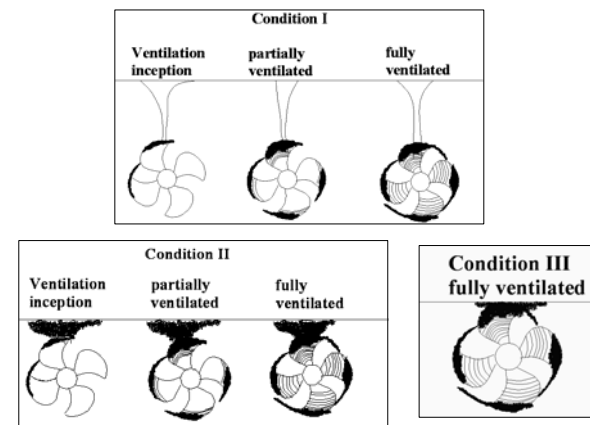


Figure 6 Different ventilation regimes for Conditions I, II & III ventilation inception, partial ventilation, full ventilation.

Figures 7-12 present the photographs of different ventilation regimes with respect to time for bollard condition.

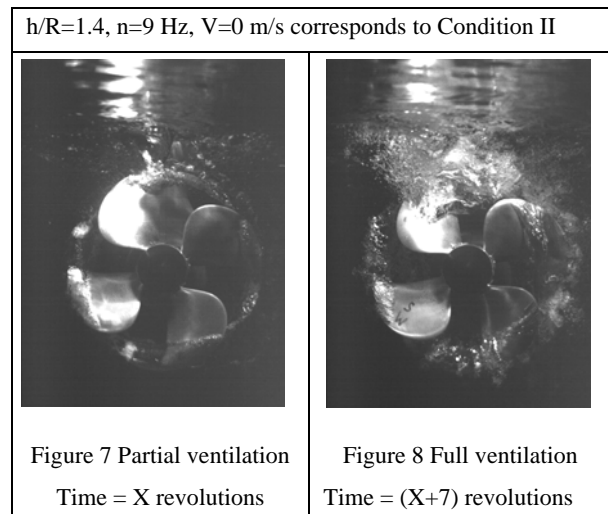


Figure 7 Partial ventilation  
Time = X revolutions

Figure 8 Full ventilation  
Time = (X+7) revolutions

$h/R=2.6, n=14 \text{ Hz}, V=0 \text{ m/s}$  corresponds to Condition I

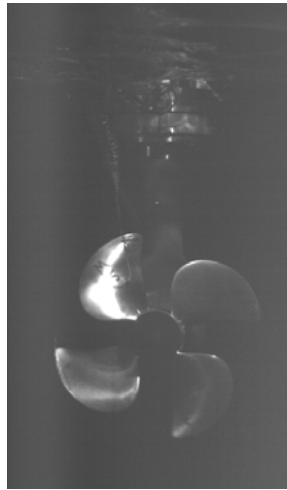


Fig. 9 Ventilation inception  
Time = X revolutions

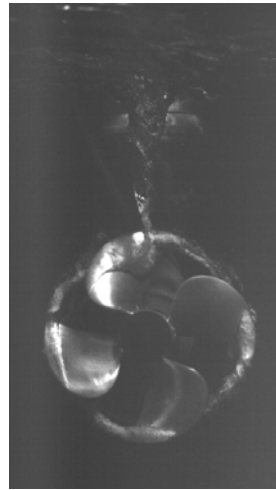


Fig. 10 Partial ventilation  
Time=(X+23) revolutions

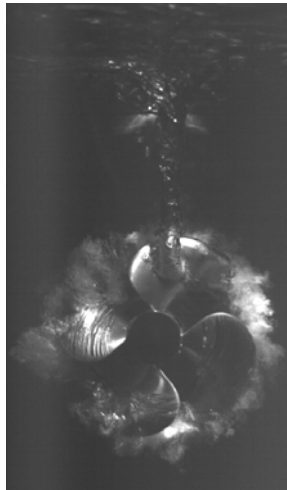


Fig. 11 Transition region  
Time=(X+26) revolutions

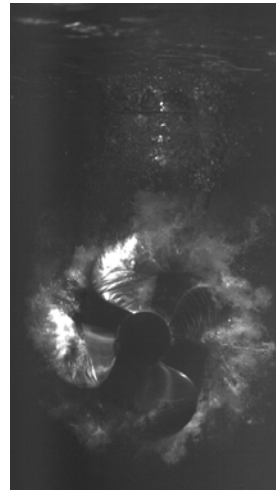


Fig. 12 Full ventilation  
Time=(X+28) revolutions

The photographs above show that the time between ventilation inception and full ventilation increases with submergence of the propeller. For propeller submergence ratio equal to 2.4 the time period from ventilation inception to full ventilation is three times larger than for propeller immersion ratio equal to 1.4.

## 6 MEAN THRUST AND TORQUE LOSSES

Thrust and torque loss factors are defined as follows:

$$\beta_T = \frac{T_t}{T_n} \quad (9)$$

$$\beta_Q = \frac{Q_t}{Q_n} \quad (10)$$

Where:  $T_n = K_{Tn} \rho n^2 D^4$  (11)

$$Q_n = K_{Qn} \rho n^2 D^5 \quad (12)$$

$\beta_T, \beta_Q = 1$  means no thrust or torque loss and  $\beta_T, \beta_Q = 0$  means total thrust or torque loss due to ventilation and out of water effects.

In Figure 13 the total thrust loss is plotted as a function of the submergence ratio and the shaft speed, the advance ratio is equal to zero (bollard condition).

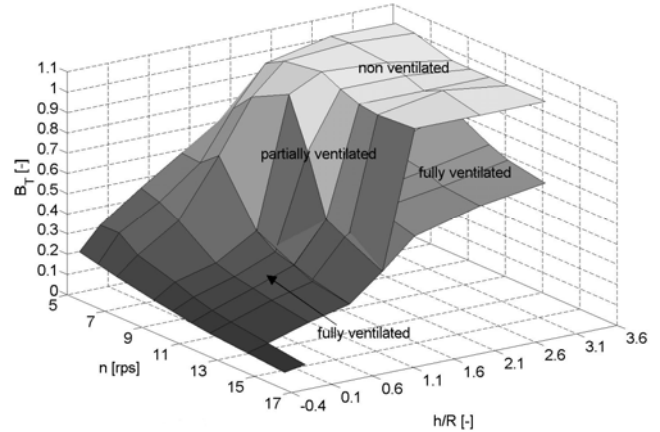


Figure 13 Thrust loss

In Figure 14 the total torque loss is plotted as a function of the submergence ratio and the shaft speed, the advance ratio is equal to zero (bollard condition).

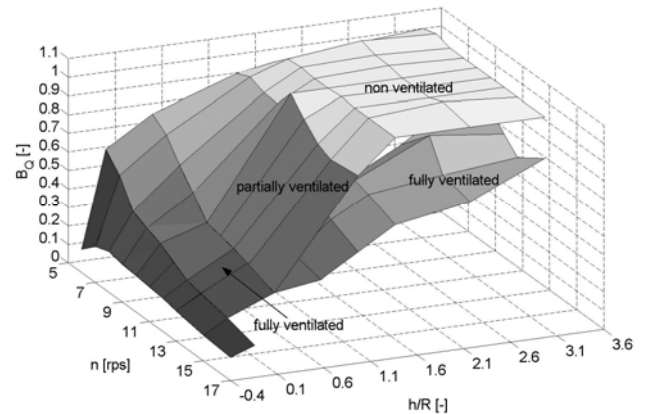


Figure 14 Torque loss

Since ventilation is a time dependent phenomena we divide the thrust and torque loss factors in two areas. It means that especially for large submergences the propeller can either ventilate or not. It depends on the duration of the experiments. Based on observation we can separate the experimental results in the following regimes: for propeller submergence above  $h/R=1.8$  we can observe both non ventilated or ventilated regime (condition I in chapter 4), for propeller submergence within  $1 < h/R < 1.8$  we observe either partially ventilated or fully ventilated regime (conditions I & II in chapter 4), and below propeller submergence  $h/R=1$  we have only fully ventilated case (condition III in chapter 4). It means that we have two different thrust losses depending in which regime the propeller operates. For example the typical thrust loss for  $h/R=2.6$  is 30% for ventilated case and 0% for non ventilating regime. For  $h/R=1.4$  the typical thrust loss is 75% for fully ventilated area and 50% for partially ventilated case. When the propeller submergence is less than  $h/R=1$  we observe thrust loss equal to 80% due to ventilation and out of water effect.

The propeller torque (illustrated in Figure 14) has similar behavior as propeller thrust and shows good agreement with experimental results by Minsaas (1983), where:

$$K_{T_t} = \beta_T \cdot K_{T_n}, K_{Q_t} = \beta_T^m \cdot K_{Q_n} \quad (13)$$

$m$  is a constant between 0.8 and 0.85 (Minsaas 1983)

This means that if the torque is measured, one can fairly accurately know the thrust also in ventilating condition.

## 7 THRUST LOSS CALCULATIONS

For fully ventilated propellers by assuming that suction side of the propeller blade section is covered by air and pressure on the pressure side of the propeller blade section is equal to the static pressure the lift can be expressed by analogue to the lift of a cavitating foil.

$$c_{LV} = c_L(\sigma_V = 0) + \sigma_V \quad (14)$$

Where  $c_L(\sigma_V = 0)$  is the pressure side contribution at the ventilation number equal to zero which corresponds to fully ventilated case. By assuming that pressure side of the profile has no camber the lift coefficient is expressed as follows

$$c_L(\sigma_V = 0) = \frac{\pi}{2} \alpha \quad (15)$$

Due to pressure difference between the static pressure on the pressure side and the atmospheric pressure on the suction side we get the lift coefficient (excluding effect of camber and angle of incidence) as follows:

$$\sigma_V = \frac{2gh}{V_\infty^2} \quad (16)$$

Finally the lift coefficient for fully ventilated propeller blade section can be estimated by:

$$c_{LV} = c_L(\sigma_V = 0) + \sigma_V = \frac{\pi}{2} \cdot \alpha + \frac{2gh}{V_\infty^2} \quad (17)$$

The thrust coefficient of a typical propeller can roughly be approximated by:

$$K_T = 1.5EAR \cdot c_L(0.7) \quad (18)$$

Acc. to Minsaas (1983), the thrust loss for a fully ventilated propeller may be approximated as follows:

$$\beta_V = \frac{1.5EAR}{K_{T_n}} \cdot \left( \frac{\pi}{2} \cdot \alpha + \frac{2gh}{V_\infty^2} \right) \quad (19)$$

The typical thrust loss is not only a function of ventilation. We can separate thrust loss as follows: thrust loss due to loss of propeller disc area, thrust loss due to wave making by propeller as well as ventilation and Wagner effect. The Wagner effect (Wagner, 1925) is the effect that at sudden immersion of a foil or propeller blade, the lift is just half of the steady lift. The lift grows (rapidly) with time, and converges towards the steady lift. The growth of the lift is expressed in equation 21 as a function of the number of chord lengths traveled after immersion. The thrust loss factors are summarized in equations (20-23).

1. Loss of propeller disc area: for  $h/R < 1$  can be estimated from Fleischer (1973) as follows:

$$\beta_0 = 1 - \frac{\arccos\left(\frac{h}{R}\right)}{\pi} + \frac{h}{\pi R} \sqrt{1 - \left(\frac{h}{R}\right)^2} \quad (20)$$

2. Wagner effect: for  $h/R \leq 0.7$

$$\beta_W = 0.5 + 0.5 \sqrt{1 - \left(\frac{155 - V_\infty \cdot t/c}{155}\right)^{27.59}} \quad (21)$$

Where  $V_\infty \cdot t/c$  mean the number of chord lengths to be traveled by a section ( $0.7 R$ ) between entering and leaving the water.

3. Thrust loss due to wave making by propeller.

When the propeller is working close to the free surface we observe the diminution of propeller thrust due to the wave set up by the propeller. Thrust loss factors due to the wave making by propeller as well as loss of propeller disc area and Wagner effect were discussed by Faltinsen (1981) and Minsaas (1983). As a result a total thrust loss factor  $\beta$  without the effect of ventilation was developed.

Acc. to Minsaas (1983) the  $\beta$  curve may be approximated as follows:

$$\beta = 1 - 0.657[1 - 0.0769(h/R)]^{1.258} \quad \text{for } h/R < 1.3 \quad (22)$$

Where:  $\beta$  - total thrust loss factor without the effect of ventilation

4. Ventilation: see equation 19

As a result total thrust diminution factor can be expressed as follows:

$$\beta_T = \beta_V \cdot \beta \quad (23)$$

In Figure 15 both experimental and calculated total thrust loss factors for fully ventilated regime are plotted as a function of submergence for different advance ratios i.e.  $J = -0.1, 0.1$  &  $0$  and constant prop. revolution  $n = 14\text{Hz}$ .

Figure 16, 17 & 18 show both calculated and experimental total thrust losses for fully ventilated regime as a function of submergence and propeller rate of revolutions in three different advance ratios.

All of these figures (15, 16, 17, & 18) show that for low submergences ( $h/R < 0.5$ ) the agreement between the experimental results and calculations is quite good. For propeller submergences within  $0.5 < h/R < 1.6$ , it can be seen that the calculated thrust loss factor are larger than experimental values. The reason for this is unknown but it could be that the approximation of thrust diminution factor (see eq. 22) is not satisfactory since this factor can vary with propeller loading, advance velocity and rate of revolutions. For larger submergences ( $h/R > 2$ ) we see that the calculations (except for some bollard conditions) overpredict the thrust loss compared to the model tests. The reason for this is also not known, but a cause could be that in the experiments, the propeller is actually not fully ventilated for the large submergences.

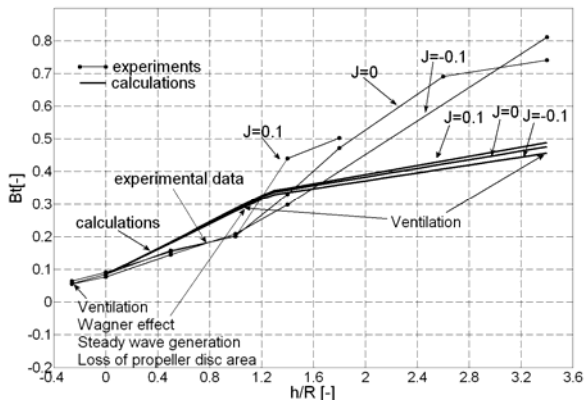


Figure 15 Comparison between calculated and experimental thrust loss factors different advance ratios

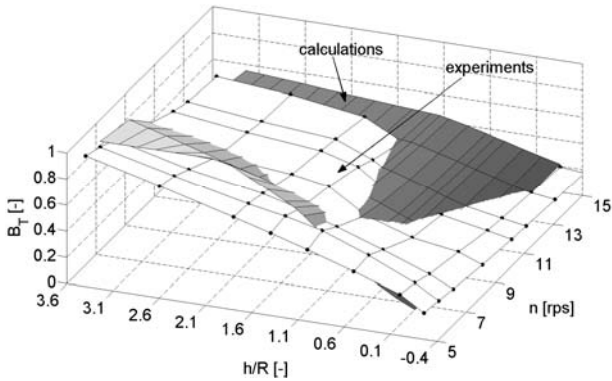


Figure 16 Comparison between calculated and experimental thrust loss factors for bollard condition

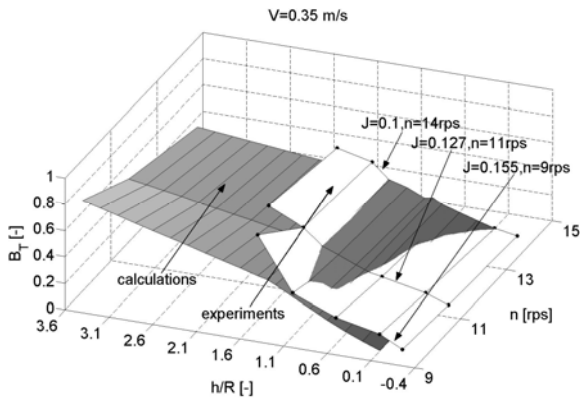


Figure 17 Comparison between calculated and experimental thrust loss factors for low positive advance ratios

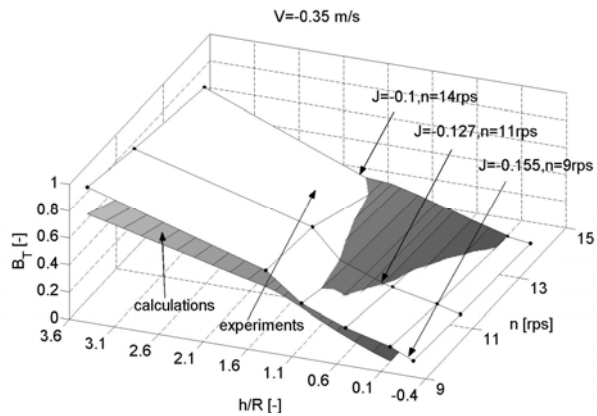


Figure 18 Comparison between calculated and experimental thrust loss factors for low negative advance ratios

## 8 THRUST LOSS DUE TO BLADE POSITIONS

By following one blade during one cycle of ventilation we can find the relation between different types of ventilation and typical thrust loss. It is worth mentioned that both experimental data in undisturbed condition (corresponds with deeply submerged propeller and no ventilation) as well as if the ventilation appears show oscillations in the blade frequency range most notably  $n$  and  $4n$  (shaft and blade frequency). Since these oscillations also appear for deeply submerged, non ventilated propeller it means that they are probably not cause by ventilation. The oscillations at  $4n$  could be caused by mechanical or measurement noise, or flow phenomena like interaction between the blade tip vortices. Since there has not been found any precise explanation of this phenomenon the experiments are presented both in original and filtered format. Measurement data was filtered by using FFT (Fast Fourier Transform) in Matlab. The low pass filter is used for this analysis and the filtered frequency is less than 4 times propeller frequency ( $f < 4n$ ). In Figure 19 the superposition of individual blade loading histories from 0 to 360 deg is presented as a function of thrust loss in different submergence ratios. We present one blade revolution which is the mean value for every blade revolution during one test.  $FX$ -denotes the time averaged axial force for a single blade in ventilated condition and  $FX0$ -denotes the time averaged axial force of a single blade for non ventilated condition.

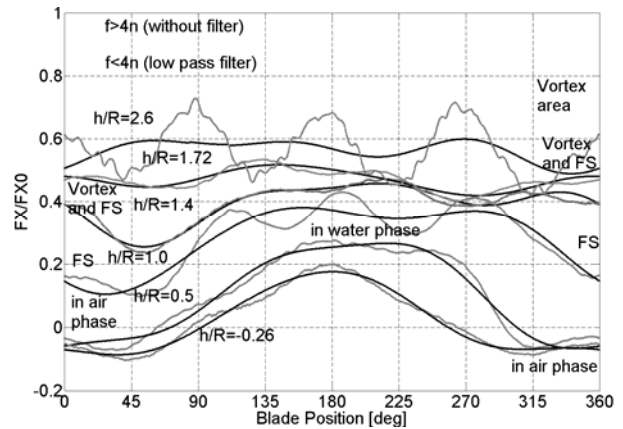


Figure 19 Thrust losses as a function of blade position for original and filtered experimental data,  $n=14\text{Hz}$ ,  $V=0\text{m/s}$

For the propeller submergence equal to 2.6 the air filled vortex reaches the blade in blade position 315-360 deg and we observed the largest thrust drop at blade position equal to 315 for original and 330 for filtered experimental data. For propeller submergence equal to 1.4 at 60 deg (both for original and filtered data) we observe a large thrust drop which can be related to the vortex funnel and free surface which is sucked down to the propeller (as illustrated in Figure 20). The thrust is built up again due to losing connection with the vortex and free surface after the blade passes the position of 90 deg. A similar situation occurs for propeller submergence equal to 1.0. For less submergence than 1.0 the propeller is coming out of the water and we observe large thrust loss, which is connected with loss of propeller disc area. The thrust

builds up again during the in-water phase and can achieve 25% of nominal thrust for  $h/R=0.5$  and 18% for  $h/R = -0.26$ .

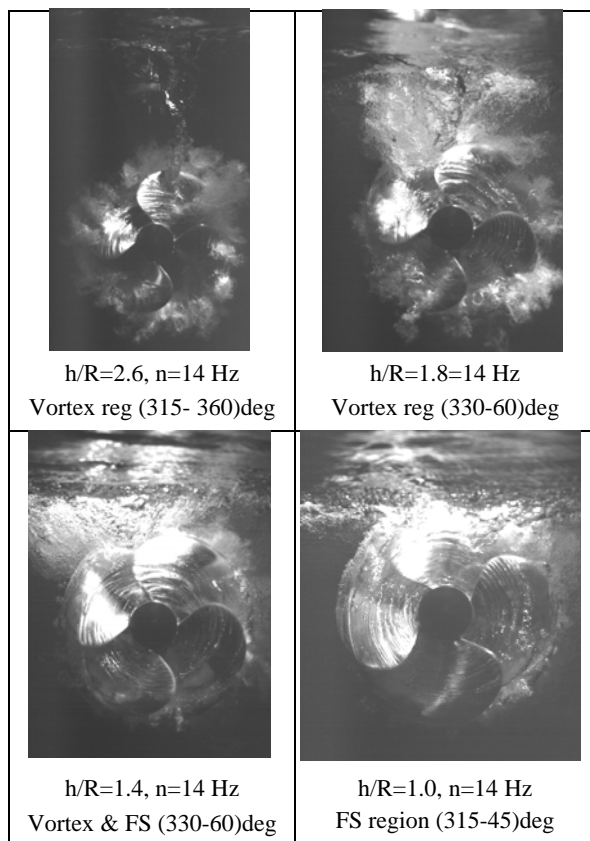


Figure 20 Ventilation for several propeller submergence ratios at bollard condition

## 9 CONCLUSIONS

New analysis has been done based on a series of experiments performed by Koushan (2006 I and II). The influence of several factors on ventilation and thrust loss were investigated. Based on the new analysis the following conclusions have been drawn:

1. We observe the three different types of ventilation inception mechanism: 1<sup>st</sup> - ventilation starts by forming an air filled vortex from the free surface, 2<sup>nd</sup> - ventilation inception is hard to observe, it probably starts by forming a vortex which is not well visible, 3<sup>rd</sup> - ventilation starts by sucking down the free surface without forming a vortex.
2. It was shown that several factors i.e. advance ratios, propeller revolutions, submergences and time have influence on ventilation inception and thrust drop due to ventilation.
3. We found reasonably good agreement between calculation of thrust loss based on empirical equations and experimental values, which means that one can roughly predict thrust loss related to ventilation and out of water effect based on empirical formulas presented in this paper. The current formula underestimates the thrust loss when the propeller works near the free surface and overpredicts the thrust loss for deeply submerged propellers. The reason for this is not known and a future

research into different types of ventilation and thrust loss related to them is planned.

4. It was shown that the propeller torque loss has similar behavior as propeller thrust loss also in ventilation condition.

## 10 ACKNOWLEDGEMENT

This work has been carried out at the University Technology Centre of Rolls Royce at NTNU as a part of "SeaPro" project, sponsored by the Rolls Royce Marine and the Research Council of Norway.

## REFERENCES

- Faltinsen, O., Minsaas, K., Liapias, N., Skjørdal, S.O. (1981). 'Prediction of Resistance and Propulsion of a Ship in a Seaway'. Proceedings of 13th Symposium on Naval Hydrodynamics, Edited by T.Inui, The Shipbuilding Research Association in Japan.
- Fleischer, K.P. (1973). 'Untersuchungen über das Zusammenwirken von Schiff und Propeller bei tilgetauchten Propellern', Publication 35/75 of Forschungszentrum des Deutschen Schiffbaus, Hamburg, Germany.
- Kempf, G. (1933). 'Immersion of Propeller', T.NEC, Vol. 50.
- Koushan, K. (2006 I). 'Dynamics of Ventilated Propeller Blade Loading on Thrusters', World Maritime Technology Conference, London, U.K.
- Koushan, K. (2006 II). 'Dynamics of Ventilated Propeller Blade Loading on Thrusters Due to Forced Sinusoidal Heave Motion', 26<sup>th</sup> Symp. On Naval Hydrodynamics Rome, Italy.
- Koushan, K. (2006 III). 'Dynamics of Propeller Blade and Duct Loadings on Ventilated Ducted Thrusters Operating at Zero Speed', Proceedings of T-Pod conference 2006, Conference held at L'ABER WRAC'H.
- Minsaas, K., Wermter, R., and Hansen, A.G. (1975). 'Scale Effects on Propulsion Factors', 14<sup>th</sup> International Towing Tank Conferences, Proceedings Volume 3.
- Minsaas, K., Faltinsen O., Person, B. (1983). 'On the Importance of Added Resistance, Propeller Immersion and Propeller Ventilation for Large Ships in a Seaway' Proc. of 2<sup>nd</sup> Int. Symp. on Practical Design in Shipbuilding (PRADS), Tokyo& Seoul. pp.149-159.
- Olofsson N. (1996). 'Force and Flow Characteristic of a Partially Submerged Propeller', Ph.D. thesis, Chalmers University of Technology, Goteborg.
- Shiba, H. (1953). 'Air - Drawing of Marine Propellers' Transportation Technical Research Institute, Report no. 9, Japan
- Wagner, H. (1925). 'Über die Entstehung des dynamischen Auftriebes vom Tragflügel' Z.f.a.MM, Vol.5.Heft 1. Feb. 1925, pp.17-35.